Isovector dipole resonance and shear viscosity in low energy heavy-ion collisions

C. Q. Guo,[1,2] Y. G. Ma,[1,3,*] W. B. He,[1,†] X. G. Cao,[1] D. Q. Fang,[1] X. G. Deng,[1] and C. L. Zhou[1,‡]

[1]*Shanghai Institute of Applied Physics, Chinese Academy of Sciences, Shanghai 201800, China*

[2]*University of Chinese Academy of Sciences, Beijing 100049, China*

[3]*ShanghaiTech University, Shanghai 200031, China*

(Received 8 August 2016; revised manuscript received 2 March 2017; published 31 May 2017)

The ratio of shear viscosity over entropy density in low energy heavy-ion collision has been calculated by using the Green-Kubo method in the framework of an extended quantum molecular dynamics model. After the system almost reaches a local equilibration for a head-on $^{40}Ca + ^{100}Mo$ collision, thermodynamic and transport properties are extracted. Meanwhile, the isovector giant dipole resonance (IVGDR) of the collision system also is studied. By the Gaussian fits to the IVGDR photon spectra, the peak energies of the IVGDR are extracted at different incident energies. The result shows that the IVGDR peak energy has a positive correlation with the ratio of shear viscosity over entropy density. This is a quantum effect and indicates a difference between nuclear matter and classical fluid.

DOI: 10.1103/PhysRevC.95.054622

I. INTRODUCTION

Shear viscosity, as an important transport coefficient of fluids, attracted more attention in recent years [1–4]. Some years ago, Kovtun, Son, and Starinets (KSS) found [5] that the ratio of shear viscosity η over the entropy density s has a low limit bound for all fluids, namely, the value,

$$\frac{\eta}{s} \geqslant \frac{1}{4\pi}, \tag{1}$$

in certain supersymmetric gauge theories. The value of $\frac{1}{4\pi}$ was claimed as the universal lower bound of shear viscosity over entropy density, i.e., the so-called KSS bound. The lower the η/s is, the more ideal the fluid behaves. The analysis of the ultrarelativistic heavy-ion collisions from the Relativistic Heavy Ion Collider (RHIC) seems to indicate that the strongly interacting quark-gluon matter behaves like a perfect liquid with the above ratio being close to the lower limit [6]. Many experimental efforts at the RHIC and the Large Hadron Collider (LHC) as well as theoretical investigations have been carried out for the study of η/s of this extreme hot and dense quark matter. Along this direction, the temperature dependence of η/s has been studied in high energy heavy-ion collisions [7] by comparing with the LHC and RHIC data where the partonic fluid is almost ideal. However, in heavy-ion collisions at very low energies, a nucleus behaves like a Fermi nucleonic fluid rather than a partonic fluid, and the related study of η/s of the nuclear matter is very limited. In this context, studies of the behavior of η/s of nuclear matter at low temperatures is very interesting through low energy heavy-ion collisions [8–10].

Some previous studies have investigated the shear viscosity over entropy density for warm nuclear matter in various models, such as for an equilibrated system of nucleons and fragments produced in multifragmentation within an extended statistical multifragmentation model [11] for an evolving system with the nuclear transport models [8,9,12–15] and thermal models [16], etc. Studies also focus on the η/s behavior when the nuclear liquid-gas phase transition [17–20] takes place where a local minimum of η/s is found [8,11,14–16].

Meanwhile, η/s of low excited nuclear matter also was touched by a probe of dipole resonance in the lower excitation energy region [21,22]. Fluid viscosity always plays an important role in the collective motions of fluids. For instance, wave propagation velocity and damping are dependent on fluid viscosity. However, wave frequency is independent of fluid viscosity. When a wave propagates into different kinds of fluids, the frequency remains unchanged. Giant resonance is a kind of collective motion built in nuclei, and the relation between giant resonance and nuclear matter viscosity is interesting and worth studying. On the width of giant dipole resonance (GDR), it consists of the Landau width Γ^{LD} [23], the spreading width $\Gamma^{\downarrow}$ [24], and the escape width $\Gamma^{\uparrow}$. For medium and heavy nuclei, the spreading width $\Gamma^{\downarrow}$ gives the major contribution, which corresponds to two-nucleon interaction. The dependence of the giant dipole resonance width on the shear-viscosity over the entropy-density ratio has been discussed [22]. In terms of macroscopic description, the isovector giant dipole resonance (IVGDR) is considered as a collective motion in which all the protons and neutrons, respectively, moving together with opposite phase positions [25] as shown in Fig. 1. Two components of nuclear matter, protons and neutrons, moving against each other, form a dipole oscillation which is different from classical waves in a fluid. From this classical description, the viscosity of nuclear matter should affect the frequency of the IVGDR because strong viscosity may slow down the frequency of a dipole oscillation between the neutrons' centers and the protons' centers. The frequency of a dipole resonance nuclear system is represented by the peak energy of the GDR. Therefore, the viscosity may be inversely proportional to the peak energy of the GDR. However, the

*Corresponding author: ygma@sinap.ac.cn

†Present address: Institute of Modern Physics, Fudan University, Shanghai 200433, China.

‡Present address: Shanghai United Imaging Healthcare Co., Ltd., Shanghai 201807, China.

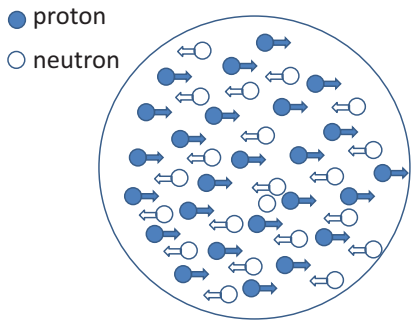

FIG. 1. A schematic for the macroscopic description of the isovector giant dipole resonance.

relation between the viscosity of nuclear matter and the peak energy (or frequency) of the isovector dipole oscillation is not clear so far, and it deserves a detailed investigation.

Heavy-ion collision is an efficient tool for investigating nuclear matter properties from low energy to relativistic energy. In heavy-ion fusion with low energy collisions, the relation between the temperature of nuclear matter and the width of the giant resonance spectra is confirmed [26,27]. In contrast, temperature dependence of the frequency of neutron-proton oscillations indicated by the giant resonance spectra is not so clear. Of course, some experiments and model calculations show that the giant resonance spectra move to low energy when the temperature of nuclear matter gets higher [28,29]. To discuss the viscosity dependence of the frequency of the isovector dipole oscillation, heavy-ion collisions provide an ideal venue.

In this paper, an extension version of the quantum molecular dynamics model is employed to calculate ^{40}Ca + ^{100}Mo head-on collisions. The thermodynamic and transport properties are extracted from the nuclear fireball located in the central sphere with the radius of $R = 3$ fm. The rest of the paper is organized as follows. Section II provides a brief introduction of an extended quantum molecular dynamics (EQMD) model, a formula of thermodynamic properties, the shear viscosity by the Green-Kubo method, as well as the GDR spectrum. The relation of shear viscosity and GDR peak energies also is presented in this section. Finally a summary is given in Sec. III.

II. MODEL AND RESULTS

A. An extended quantum molecular dynamics model

The QMD model [30,31] approach is a many-body theory describing heavy-ion collisions in ten to GeV per nucleon range. Later on an EQMD model in which the width of the Gaussian wave packets for each nucleon is independent and treated as a dynamical variable [32,33]. Furthermore, the Pauli potential is employed in the EQMD model [32] and plays an important role to describe some special structures, such as α clustering in light nuclei [34], which is a current hot topic in nuclear structure physics [35–37]. In the EQMD, each nucleon in a colliding system is described as a Gaussian wave packet,

$$\phi_i(\mathbf{r}_i) = \left(\frac{\nu_i + \nu_i^*}{2\pi}\right)^{3/4} \exp\left[-\frac{\nu_i}{2}(\mathbf{r}_i - \mathbf{R}_i)^2 + \frac{i}{\hbar}\mathbf{P}_i \cdot \mathbf{r}_i\right]. \tag{2}$$

Here $\mathbf{R}_i$ and $\mathbf{P}_i$ are the central parts of the wave packet in coordinate space and in momentum space, respectively. The complex Gaussian width ν_i is

$$\nu_i = \frac{1}{\lambda_i} + i\delta_i. \tag{3}$$

Here, λ_i and δ_i are the real part and the imaginary part, respectively, of the wave packet. The single nucleon density $[\rho_i(\mathbf{r},t)]$, matter density $[\rho(\mathbf{r},t)]$ in coordinate space, and the kinetic-energy density $[\rho_k(\mathbf{r},t)]$ in momentum space, respectively, can be calculated by the sum over all nucleons by the following equations:

$$\rho_i(\mathbf{r},t) = \frac{1}{(\pi\lambda_i)^{3/2}} \exp\left[-\frac{(\mathbf{r}^2 - \mathbf{r}_i^2)}{\lambda_i}\right], \tag{4}$$

$$\rho(\mathbf{r},t) = \sum_{i=1}^{A_T+A_P} \rho_i(\mathbf{r},t), \tag{5}$$

$$\rho_k(\mathbf{r},t) = \sum_{i=1}^{A_T+A_P} \frac{\mathbf{P}_i(t)^2}{2m}\rho_i(\mathbf{r},t). \tag{6}$$

The total wave function of the system is a direct product of the Gaussian wave packets of nucleons,

$$\psi = \prod_i \phi_i(\mathbf{r}_i). \tag{7}$$

The Hamiltonian is written as

$$H = \langle\Psi| \sum_i -\frac{\hbar^2}{2m}\nabla_i^2 - T_{\text{c.m.}} + H_{\text{int}}|\Psi\rangle \tag{8}$$

$$= \sum_i \left[\frac{\mathbf{P}_i^2}{2m} + \frac{3\hbar^2(1+\lambda_i^2\delta_i^2)}{4m\lambda_i}\right] - T_{\text{c.m.}} + H_{\text{int}}, \tag{9}$$

where $T_{\text{c.m.}}$ and H_{int} denote the spurious zero-point center-of-mass kinetic-energy and the potential-energy terms, respectively. For the effective interaction H_{int}, we use Skyrme, Coulomb, symmetry, and the Pauli potential, i.e.,

$$H_{\text{int}} = H_{\text{Skyrme}} + H_{\text{Coulomb}} + H_{\text{symmetry}} + H_{\text{Pauli}}. \tag{10}$$

Specifically, the Pauli potential is written as

$$H_{\text{Pauli}} = \frac{c_P}{2}\sum_i (f_i - f_0)^\mu \theta(f_i - f_0), \tag{11}$$

where $f_i \equiv \sum_j \delta(S_i,S_j)\delta(T_i,T_j)|\langle\phi_i|\phi_j\rangle|^2$ is the overlap of a nucleon i with nucleons having the same spin and isospin and θ is the unit step function. The coefficient c_P is the strength of the Pauli potential.

Time evolutions of the nuclear matter density and kinetic-energy density in a central volume ($R = 3$ fm) are shown in Fig. 2. At different energies, both the nuclear density and the kinetic-energy density display rapid growth at the beginning,

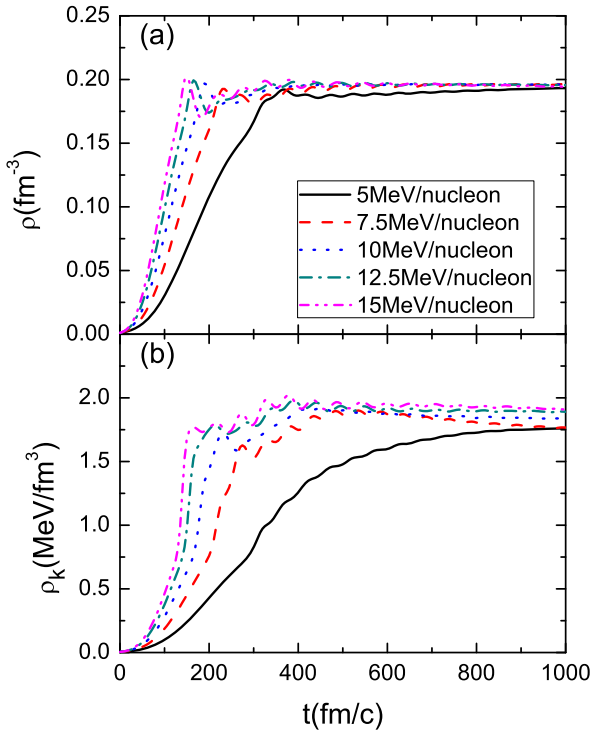

FIG. 2. (a) The time evolution of the nuclear matter density and (b) kinetic-energy density within a central volume ($R = 3$ fm) for the head-on ^{40}Ca + ^{100}Mo collisions. The different color lines represent different incident energies.

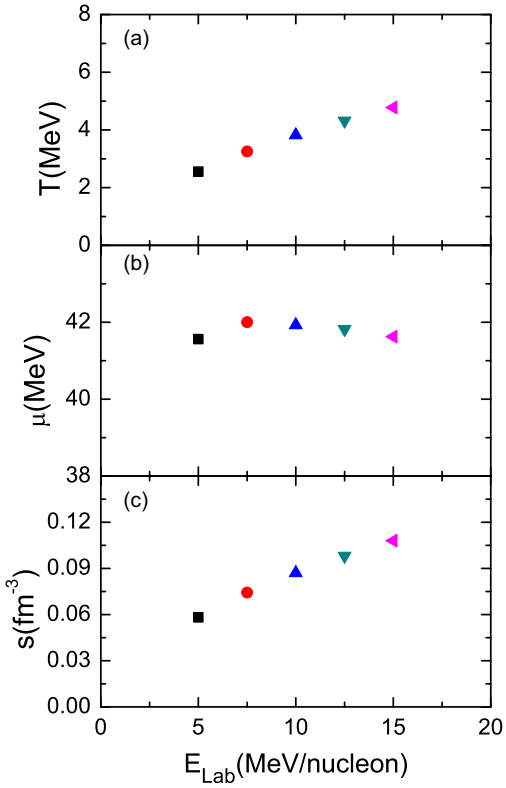

FIG. 3. (a) The temperature, (b) the chemical potential, and (c) the entropy density of the compound nucleus in a central region at different incident energies.

then the densities of the nuclear system have a small shock until they approach equilibrium due to the fusion(like) reaction mechanism.

B. Formula of thermodynamic properties

Thermodynamical properties of hot nuclear matter formed in heavy-ion collisions, e.g., temperature, chemical potential, and entropy density, can be extracted by different approaches.

At low temperatures, $T \ll \varepsilon_F$ (ε_F is the Fermi energy), the relation between the excitation energy E^* and the temperature T is given by

$$E^* = aT^2. \tag{12}$$

For the expression of the level density the Reisdorf formalism [38] is used with a value of the parameter a for $A/8$ in our calculation. When the fusion reaction is close to the stable state, we assume that the compound nucleus is uniformly heating, so the temperature of the central region is the same as the entire system.

The average temperature of the compound system in a central sphere is shown in Fig. 3(a). With the incident energy increasing, the nuclear temperature increases slightly.

The chemical potential μ_i of the nucleon in the model can be determined by the following implicit equation:

$$\frac{1}{2\pi^2}\left(\frac{2m}{\hbar^2}\right)^{3/2}\int_0^\infty \frac{\sqrt{e_k}}{\exp\left(\frac{e_k-\mu_i}{T}\right)+1}de_k = \rho_i, \tag{13}$$

where $e_k = \frac{p^2}{2m}$ is the kinetic energy and p is the momentum of the nucleons [14]. Therefore, using this formula, one can calculate the chemical potential by the nucleon's information, e.g., momentum, density, and temperature. The chemical potential in a central sphere when the system almost reaches a local equilibration is shown in Fig. 3(b).

For the entropy density calculation, it is straightforward to derive the entropy after the density, temperature, and the chemical potential have been determined [39]

$$S \equiv \frac{U-A}{T} = \bar{N}\left[\frac{5}{2}\frac{f_{5/2}(z)}{f_{3/2}(z)} - \ln z\right], \tag{14}$$

where $\bar{N}$ is the number of nucleons. $f_m(z) = \frac{1}{\Gamma(m)}\int_0^\infty \frac{x^{m-1}}{z^{-1}e^x+1}dx$ and $z = e^{\mu/T}$ is the fugacity. For transforming entropy (S) and entropy density (s), we have

$$s = \frac{\rho}{\bar{N}}S = \rho\left[\frac{5}{2}\frac{f_{5/2}(z)}{f_{3/2}(z)} - \ln z\right]. \tag{15}$$

C. Ratio of shear viscosity over entropy density by the Green-Kubo formula

As mentioned above, we need to check if the equilibrium of the collision system has been reached before a Green-Kubo formula can be applied. To this end, we use a stopping

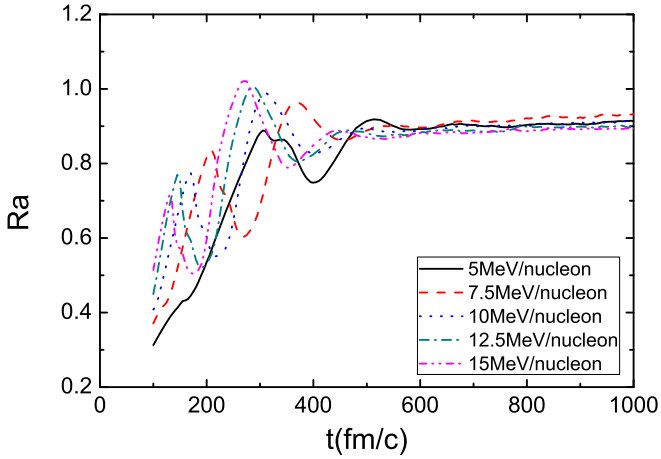

FIG. 4. The time evolution of the stopping parameter in a central region at different incident energies.

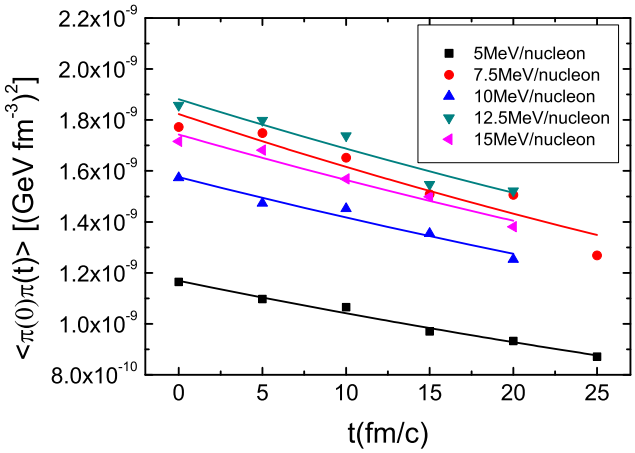

FIG. 5. The postequilibration time evolution of the stress tensor in a central region at different incident energies.

parameter R_a [40], which is defined as

$$R_a = \sum_{i=1}^{A} \frac{2\sqrt{p_x^2 + p_y^2}}{\pi \sqrt{p_z^2}} \tag{16}$$

for checking the degree of the equilibrium. The time evolution of R_a in a central volume shown in Fig. 4 illustrates that the R_a approaches a saturated value close to 1, which means the nuclear system in the central region is close to equilibrium in the later stage of the collisions.

To study the extended irreversible dynamic processes, the Kubo fluctuation theory is employed to extract transport coefficients. Shear viscosity determines the strength of the energy momentum fluctuation of dissipative fluxes around the equilibrium state, which can be calculated by the Green-Kubo relation. The Green-Kubo formula [41] for shear viscosity is defined by

$$\eta = \frac{1}{T} \int d^3r \int_0^\infty dt \langle \pi_{ij}(0,0)\pi_{ij}(\mathbf{r},t)\rangle, \tag{17}$$

where T is the equilibrium temperature of the system, t is the postequilibration time (0 represents the starting time when the system tends to equilibrium), and $\langle \pi_{ij}(0,0)\pi_{ij}(\mathbf{r},t)\rangle$ is the shear component of the energy momentum tensor. The expression for the energy momentum tensor is defined by $\pi_{ij} = T_{ij} - \frac{1}{3}\delta_{ij} T_i^i$ where the momentum tensor is written as [10]

$$T_{ij}(\mathbf{r},t) = \int d^3p \frac{p^i p^j}{p^0} f(\mathbf{r},\mathbf{p},t), \tag{18}$$

where p^i, p^j is the momentum component and p^0 is the total energy of each nucleon, $f(\mathbf{r},\mathbf{p},t)$ is the phase-space density of the particles. To compute an integral, we assume that nucleons are uniformly distributed inside the volume. Meanwhile, the spherical volume with the radius of $R = 3$ fm is fixed, so the viscosity becomes

$$\eta = \frac{V}{T} \langle \pi_{ij}(0)^2 \rangle \tau_\pi, \tag{19}$$

where τ_π represents the relaxation time and can be extracted from the following fit:

$$\langle \pi_{ij}(0)\pi_{ij}(t)\rangle \propto \exp\left(-\frac{t}{\tau_\pi}\right). \tag{20}$$

As shown in Fig. 5, $\langle \pi_{ij}(0)\pi_{ij}(t)\rangle$ is plotted as a function of time for the ^{40}Ca + ^{100}Mo collision at different incident energies. The correlation function is damped exponentially with time and can be fitted by Eq. (20) to extract the inverse slope correspondence to the relaxation time.

Finally, the shear viscosity can be obtained by Eq. (19). Figure 6 shows the ratio of shear viscosity over entropy density as a function of temperature. In low energy ^{40}Ca + ^{100}Mo collisions, as the incident energy increases, the temperature slightly increases, however, the ratio of shear viscosity over entropy density of the nuclear fireball shows a slight drop. Of

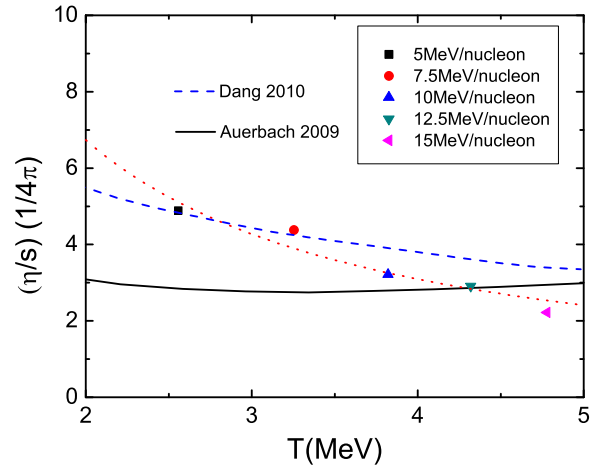

FIG. 6. The ratio of shear viscosity over entropy density as a function of temperature in a central region for the head-on ^{40}Ca + ^{100}Mo collisions. The solid line (Auerbach and Shlomo) is taken from Ref. [21], and the dashed line (Dinh Dang) is an extrapolation of the phonon-damping model prediction for ^{208}Pb in Ref. [22]. [Note the units on the vertical axis, $(1/4\pi)$].

course, this dependence trend is consistent with our previous studies [8,12]. In the same figure, two lines also are plotted for comparison. The solid line is taken from Ref. [21], which is for an ideal Fermi gas, and the dashed line is an extrapolation of the phonon-damping model prediction for ^{208}Pb of Ref. [22]. Even though the systems are not the same as ours for these giant dipole resonances in Refs. [21,22], overall, different methods do not give too many different η/s values.

D. Giant dipole resonance

The giant dipole resonance, that is formed during fusion in the N/Z asymmetry heavy-ion reactions in this paper, comes from preequilibrium dipole oscillations due to the charge asymmetry in the entrance channel, a so-called dynamical dipole mode. It is called preequilibrium GDR formed in a hot nucleus, which is different from the standard GDR that generally is excited by using rapidly varying electromagnetic fields associated with photons or generated by fast electrically charged particles [42]. For an example, the oscillation frequency of preequilibrium GDR is expected to be smaller because of the large deformation along the fusion path [42,43].

For a collision system, the isovector giant dipole moment in coordinator space $DR(t)$ and in momentum space $DK(t)$, respectively, is written [43–46] as

$$DR(t) = \frac{NZ}{A}[R_Z(t) - R_N(t)], \tag{21}$$

$$DK(t) = \frac{NZ}{A\hbar}\left[\frac{P_Z(t)}{Z} - \frac{P_N(t)}{N}\right], \tag{22}$$

where $R_Z(t)$ and $R_N(t)$ are the center of mass of the protons and neutrons, respectively, in coordinate space and $P_Z(t)$ and $P_N(t)$ are the center of mass of the protons and neutrons, respectively, in momentum space. Figure 7(a) shows the time evolution of the giant dipole oscillation in coordinate space at different incident energies. It is clear that there are dipole oscillations at different incident energies.

Derived from the overall dipole moment $D(t)$, one can get the γ-ray emission probability for energy E where the calculation formulas were introduced by Baran *et al.* in Ref. [43],

$$\frac{dP}{dE} = \frac{2}{3\pi}\frac{e^2}{E\hbar c^3}\left|\frac{d\bar{V}_k}{dt}(E)\right|^2, \tag{23}$$

where $\frac{dP}{dE}$ can be interpreted as the average number of γ rays emitted per energy unit and $\frac{d\bar{V}_k}{dt}(E)$ is the Fourier transformation of the second derivative of $DR(t)$ with respect to time,

$$\frac{d\bar{V}_k}{dt}(E) = \int_0^{t_{\max}} \frac{d^2DR_k(t)}{dt^2} e^{i(Et/\hbar)}dt. \tag{24}$$

By the above equation, the photon emission spectrum can be obtained and shown in Fig. 7(b). The results show that the frequency of the dipole oscillation is dependent on the temperature of nuclear matter. Finally, the peak energies of the IVGDR at different incident energies are extracted by the Gaussian fitting to the spectrum. Figure 7(c) displays that the energy of the peak (centroid) positions is inversely

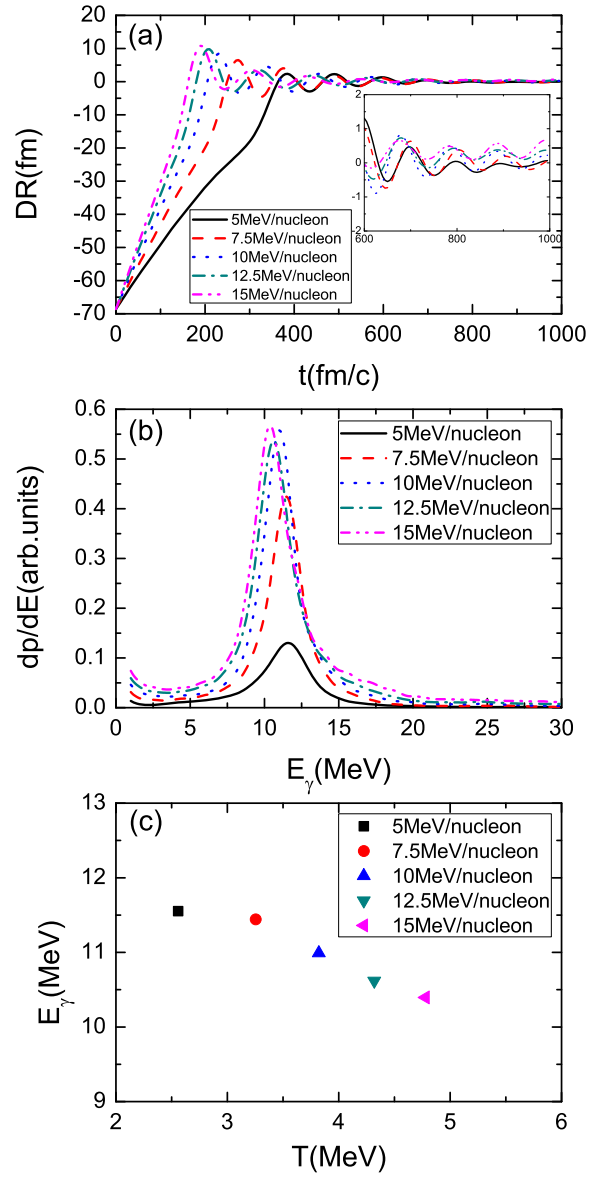

FIG. 7. The time evolution of the (a) the giant dipole moment in coordinate space, (b) the GDR spectra, and (c) their centroid energies for the head-on ^{40}Ca + ^{100}Mo collisions with different incident energies.

proportional to the temperature. This tendency is consistent with the results of previous experiments [29].

E. Relationship of the GDR and η/s

The relation between the ratio of shear viscosity over entropy density and peak energy is shown in Fig. 8. As the temperature gets higher, both the frequency of the dipole oscillation and the shear viscosity over entropy density become lower. This is very interesting since the tendency is against the prediction made from the classical description as mentioned earlier in this paper. This contradiction also indicates that the dependence between the viscosity of the nuclear matter and the frequency of the dipole oscillation is

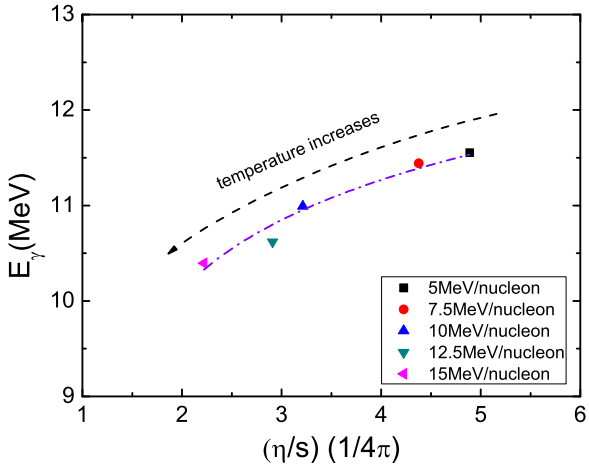

FIG. 8. The peak energy of the GDR as a function of the ratio of shear viscosity over entropy density for the head-on ^{40}Ca + ^{100}Mo collision. [Note the units on the horizontal axis, $(1/4\pi)$.]

a quantum effect, which is an important difference between nuclear matter and classical fluid.

Assuming the above dependence between the η/s and the frequency of the dipole oscillation can be extrapolated to extreme conditions of nuclear matter, one can get some interesting extrapolations. For instance, for the extremely high temperature, where quark-gluon plasma could be formed, the frequency of the dipole oscillation (assuming it still exists) will be extremely low, and the matter behaves like a nearly perfect fluid with extremely low viscosity. In other words, there is no way to get dipole excitation for a nearly perfect fluid.

III. CONCLUSION

In this article, we use an EQMD model to simulate some thermodynamic quantities for a fusion system of ^{40}Ca + ^{100}Mo at beam energies from 5 to 15 MeV/nucleon. The ratio of shear viscosity over entropy density is obtained by applying the Green-Kubo formula after the fusion system almost is equilibrated, and its value is about $\frac{(2–5)}{4\pi}$ in this energy range. Meanwhile, the IVGDR spectra are obtained for the system, and the peak energies are extracted at each incident energy (or temperature of the fusion system). From the Gaussian fits to the IVGDR spectra, the peak energy shows a slight decrease with the increasing of temperature. By temperature dependencies of both η/s and peak energies of the IVGDR, the relation of the peak energies of the IVGDR versus the ratio of shear viscosity over entropy density of the system is established, and a positive correlation was found. This behavior seems against the guess from the classical description of fluids. In this context, the η/s dependence of the frequency (peak energy) of the dipole oscillation is a kind of quantum effect.

ACKNOWLEDGMENTS

This work was supported, in part, by the National Natural Science Foundation of China under Contracts No. 11421505, No. 11220101005, and No. 11305239, the Major State Basic Research Development Program in China under Contract No. 2014CB845401, and the Key Research Program of Frontier Sciences of the CAS under Grant No. QYZDJ-SSW-SLH002.

[1] P. Danielewicz, Phys. Lett. B **146**, 168 (1984).
[2] L. Shi and P. Danielewicz, Phys. Rev. C **68**, 064604 (2003).
[3] C. Cao, E. Elliott, J. Joseph *et al.*, Science **331**, 58 (2011).
[4] C. Shen and U. Heinz, Nucl. Phys. News **25**, 6 (2015).
[5] P. K. Kovtun, D. T. Son, and A. O. Starinets, Phys. Rev. Lett. **94**, 111601 (2005).
[6] K. Adcox *et al.*, Nucl. Phys. A **757**, 184 (2005); B. B. Back *et al.*, *ibid.* **757**, 28 (2005); J. Arsene *et al.*, *ibid.* **757**, 1 (2005); J. Adams *et al.*, *ibid.* **757**, 102 (2005).
[7] G. Denicol, A. Monnai, and B. Schenke, Phys. Rev. Lett. **116**, 212301 (2016).
[8] C. L. Zhou, Y. G. Ma, D. Q. Fang, and G. Q. Zhang, Phys. Rev. C **88**, 024604 (2013).
[9] S. X. Li, D. Q. Fang, Y. G. Ma, and C. L. Zhou, Phys. Rev. C **84**, 024607 (2011); Nucl. Sci. Tech. **22**, 235 (2011).
[10] A. Muronga, Phys. Rev. C **69**, 044901 (2004).
[11] S. Pal, Phys. Rev. C **81**, 051601(R) (2010).
[12] C. L. Zhou, Y. G. Ma, D. Q. Fang, S. X. Li, and G. Q. Zhang, Europhys. Lett. **98**, 66003 (2012).
[13] C. L. Zhou, Y. G. Ma, D. Q. Fang, G. Q. Zhang, J. Xu, X. G. Cao, and W. Q. Shen, Phys. Rev. C **90**, 057601 (2014).
[14] D. Q. Fang, Y. G. Ma, and C. L. Zhou, Phys. Rev. C **89**, 047601 (2014).
[15] X. G. Deng, Y. G. Ma, and M. Veselský, Phys. Rev. C **94**, 044622 (2016).
[16] J. Xu, L. W. Chen, C. M. Ko, B. A. Li, and Y. G. Ma, Phys. Lett. B **727**, 244 (2013); J. Xu, Nucl. Sci. Tech. **24**, 050514 (2013).
[17] C. A. Ogilvie, J. C. Adloff, M. Begemann-Blaich, P. Bouissou, J. Hubele, G. Imme, I. Iori, P. Kreutz, G. J. Kunde, S. Leray, V. Lindenstruth, Z. Liu, U. Lynen, R. J. Meijer, U. Milkau, W. F. J. Müller, C. Ngô, J. Pochodzalla, G. Raciti, G. Rudolf, H. Sann, A. Schüttauf, W. Seidel, L. Stuttge, W. Trautmann, and A. Tucholski, Phys. Rev. Lett. **67**, 1214 (1991); M. B. Tsang, W. C. Hsi, W. G. Lynch, D. R. Bowman, C. K. Gelbke, M. A. Lisa, G. F. Peaslee, G. J. Kunde, M. L. Begemann-Blaich, T. Hofmann, J. Hubele, J. Kempter, P. Kreutz, W. D. Kunze, V. Lindenstruth, U. Lynen, M. Mang, W. F. J. Müller, M. Neumann, B. Ocker, C. A. Ogilvie, J. Pochodzalla, F. Rosenberger, H. Sann, A. Schüttauf, V. Serfling, J. Stroth, W. Trautmann, A. Tucholski, A. Wörner, E. Zude, B. Zwieglinski, S. Aiello, G. Immé, V. Pappalardo, G. Raciti, R. J. Charity, L. G. Sobotka, I. Iori, A. Moroni, R. Scardoni, A. Ferrero, W. Seidel, T. Blaich, L. Stuttge, A. Cosmo, W. A. Friedman, and G. Peilert, *ibid.* **71**, 1502 (1993); Y. G. Ma and W. Q. Shen, Phys. Rev. C **51**, 710 (1995).
[18] J. B. Natowitz, K. Hagel, Y. Ma, M. Murray, L. Qin, R. Wada, and J. Wang, Phys. Rev. Lett. **89**, 212701 (2002); X. Campi, J. Phys. A **19**, L917 (1986); Phys. Lett. B **208**, 351 (1988); A. Bonasera, M. Bruno, C. O. Dorso, and P. F. Mastinu, Riv. Nuovo Cimento Soc. Ital. Fis. **23**, 1 (2000).
[19] Y. G. Ma, Phys. Rev. Lett. **83**, 3617 (1999).

[20] Y. G. Ma, J. B. Natowitz, R. Wada *et al.*, Phys. Rev. C **71**, 054606 (2005).
[21] N. Auerbach and S. Shlomo, Phys. Rev. Lett. **103**, 172501 (2009).
[22] N. Dinh Dang, Phys. Rev. C **84**, 034309 (2011).
[23] C. Fiolhais, Ann. Phys. (NY) **171**, 186 (1986).
[24] J. C. Bacelar, G. B. Hagemann, B. Herskind, B. Lauritzen, A. Holm, J. C. Lisle, and P. O. Tjøm, Phys. Rev. Lett. **55**, 1858 (1985).
[25] M. Goldhaber and E. Teller, Phys. Rev. **74**, 1046 (1948).
[26] G. Enders, F. D. Berg, K. Hagel *et al.*, Phys. Rev. Lett. **69**, 249 (1992).
[27] K. Wang, Y. G. Ma, G. Q. Zhang, X. G. Cao, W. B. He, and W. Q. Shen, Phys. Rev. C **95**, 014608 (2017).
[28] G. Gervais, M. Thoennessen, and W. E. Ormand, Phys. Rev. C **58**, R1377(R) (1998).
[29] T. Baumanna, E. Ramakrishnana, A. Azharia *et al.*, Nucl. Phys. **A635**, 428 (1998).
[30] J. Aichelin, Phys. Rep. **202**, 233 (1991).
[31] C. Hartnack, R. K. Puri, J. Konopka, S. A. Bass, H. Stöcker, and W. Greiner, Eur. Phys. J. A **1**, 151 (1998).
[32] T. Maruyama, K. Niita, and A. Iwamoto, Phys. Rev. C **53**, 297 (1996).
[33] X. G. Cao, Y. G. Ma, G. Q. Zhang, H. W. Wang, A. Anastasi, F. Curciarello, and V. D. Leo, J. Phys.: Conf. Ser. **515**, 012023 (2014).
[34] W. B. He, Y. G. Ma, X. G. Cao, X. Z. Cai, and G. Q. Zhang, Phys. Rev. Lett. **113**, 032506 (2014); Phys. Rev. C **94**, 014301 (2016); W. B. He, X. G. Cao, Y. G. Ma *et al.*, Nucl. Techniques (in Chinese) **37**, 100511 (2014).
[35] W. v. Oertzen, M. Freer, and Y. Kanada-Enyo, Phys. Rep. **432**, 43 (2006).
[36] H. Horiuchi, K. Ikeda, and K. Kato, Prog. Theor. Phys. Suppl. **192**, 1 (2012).
[37] Y. Kanada-Enyo, M. Kimura, F. Kobayashi *et al.*, Nucl. Sci. Tech. **26**, S20501 (2015).
[38] W. Reisdorf *et al.*, Z. Phys. A **300**, 227 (1981).
[39] H. Zheng and A. Bonasera, Phys. Rev. C **86**, 027602 (2012).
[40] G. Q. Zhang, Y. G. Ma, X. G. Cao, C. L. Zhou, X. Z. Cai, D. Q. Fang, W. D. Tian, and H. W. Wang, Phys. Rev. C **84**, 034612 (2011).
[41] R. Kubo, Rep. Prog. Phys. **29**, 255 (1966).
[42] C. Simenel, P. Chomaz, and G. d. France, Phys. Rev. Lett. **86**, 2971 (2001).
[43] V. Baran, D. M. Brink, M. Colonna, and M. Di Toro, Phys. Rev. Lett. **87**, 182501 (2001).
[44] V. Baran, M. Cabibbo, M. Colonna *et al.*, Nucl. Phys. **A679**, 373 (2001).
[45] H. L. Wu, W. D. Tian, Y. G. Ma *et al.*, Phys. Rev. C **81**, 047602 (2010).
[46] S. Q. Ye, X. Z. Cai, D. Q. Fang *et al.*, Nucl. Sci. Tech. **25**, 030501 (2014); C. Tao, Y. G. Ma, G. Q. Zhang *et al.*, *ibid.* **24**, 030502 (2013).